Gas Adsorption Characterization of Ordered Organic−Inorganic Nanocomposite Materials

Michal Kruk and Mietek Jaroniec*

Department of Chemistry, Kent State University, Kent, Ohio 44240

Received January 31, 2001

A critical review of adsorption methods that are currently used in the characterization of ordered organic−inorganic nanocomposite materials is presented, and the adsorption methodology that is potentially useful for this characterization, but has not yet been applied, is discussed. The ordered organic−inorganic nanocomposites include surface-functionalized ordered mesoporous materials (OMMs) with siliceous frameworks (synthesized either via postsynthesis surface modification or via direct co-condensation method), periodic mesoporous organosilicas, and surfactant-containing OMMs. This review covers the methods for determination of the specific surface area and pore volume. The available methods for mesopore size analysis are critically compared and evaluated, with special emphasis on the recent developments related to the application of advanced computational methods for studying adsorption in porous media and to the direct modeling of adsorption using highly ordered surface-functionalized OMMs as model adsorbents. The review also covers adsorption methods for studying the surface properties of organic−inorganic nanocomposites, including those based on adsorption of molecules of different polarities. An emphasis is placed on the emerging opportunity for studying the surface properties of nanocomposites using low-pressure adsorption of nonpolar molecules, such as nitrogen and argon. The opportunities and challenges in adsorption characterization of specific surface sites, uniformity of coated or bonded layers, bonding density of groups on the surface, type of surface species, and so forth, are presented. Thus, this review provides an overview of adsorption studies dealing with organic−inorganic nanocomposites, a critical discussion of adsorption methods available for such studies, and some recommendations for thorough characterization of these materials using gas adsorption.

Introduction

The discovery of surfactant-templated ordered mesoporous materials (OMMs) in the early 1990s[1,2] created remarkable new opportunities in the field of synthesis and application of organic−inorganic nanocomposites (OINs) because it paved the way to nanocomposites with well-defined ordered porous structures, tailored surface properties, and framework compositions.[3,4] The family of ordered organic−inorganic nanocomposites (OOINs) currently includes OMMs with silica-based frameworks and surfaces functionalized with chemically bonded organic groups,[3] OMMs with organosilica frameworks (these materials will be referred to as periodic mesoporous organosilicas (PMOs)),[3,4] and surfactant-containing OMMs.[5]

Surface-functionalized silica-based OMMs can be synthesized via chemical modification of surfactant-free OMMs with organosilanes,[2] co-condensation of siloxane and organosiloxane precursors in the presence of surfactants,[6−10] or chemical reaction of as-synthesized (surfactant-containing) OMMs with organosilanes.[11−15] The first of these methods was originally demonstrated in 1992 for MCM-41 silica (which exhibits uniform cylindrical pores arranged in a two-dimensional (2-D) hexagonal (honeycomb) structure), whose surface was modified with trimethylsilyl groups.[2] The current widespread use of this functionalization method can largely be attributed to the vast knowledge on the reactions of the silica surface with modifying organic agents that has accumulated during the last 50 years, giving rise to many useful materials, including a wide variety of chromatographic packings.[16−18] OMMs with silica-based frameworks and organic groups on the surface can also be synthesized via co-condensation of silica precursors (such as tetraethyl orthosilicate, TEOS) and organosilica precursors (such as organotriethoxysilane) in the presence of a proper structure-directing agent. The latter can be chosen among ionic alkylammonium surfactants,[6] neutral alkylamines,[7] oligomeric surfactants,[8] and triblock copolymers.[9,10] The resulting ordered surfactant−organosilicate composite needs to be freed of surfactant to open its porosity, which can be achieved via solvent extraction[6−10] or, in certain cases, via calcination at temperatures sufficiently high to ensure quantitative surfactant removal, and yet low enough to preserve the organic groups attached to the silica framework.[19] The co-condensation approach is a combination of the surfactant templating, originally developed for purely inorganic materials, and the well-known co-condensation approach for the synthesis of disordered organosilicas with pendent organic groups,[20] and thus

* To whom correspondence should be addressed. E-mail: Jaroniec@columbo.kent.edu. Phone: (330) 672 3790. Fax: (330) 672 3816.

10.1021/cm0101069 CCC: $20.00
Published on Web 05/03/2001

shares the benefits of these two methodologies, including the pore structure uniformity, pore size adjusting capability, and tailorability of the surface properties. Another approach to the synthesis of OOINs is based on the direct reaction of as-synthesized OMMs with organosilanes. Despite the fact that the feasibility of this approach was demonstrated in 1990,[11] this methodology has not received much attention (except for the work of the Mobil scientists)[12] until recently. The last 2 years brought the realization that the modification of surfactant-containing OMMs not only leads to OOINs of structures similar to those attained via modification of surfactant-free materials but also allows one to achieve high loadings of organic groups.[13−15]

The aforementioned three approaches for the synthesis of OOINs share many attractive features. The ordered silica-based support imparts good mechanical, thermal, and chemical stability, additionally allowing for the pore size and pore structure tailoring, whereas surface organic groups allow for introduction of desired surface characteristics, such as sorption, or catalytic properties.[3] Because of that, the synthesis, characterization, and application of these materials have recently attracted much attention, resulting in the development of many potentially useful catalysts, adsorbents, and separation media.[3]

Reported for the first time in 1999, PMOs are novel materials synthesized via surfactant templating using organosilane precursors with two trialkoxysilyl groups bridged by an organic group.[21−23] After surfactant removal by extraction[21−23] or calcination (under an oxygen-free atmosphere and at sufficiently low temperature to prevent the degradation of framework organic groups),[24] PMOs exhibit ordered mesoporous voids readily accessible to various adsorbate molecules.[21−24] Unlike the previously discussed surface-functionalized silica-based materials with frameworks that exhibit only Si−O−Si linkages, PMO frameworks feature Si−R−Si linkages, where R is an organic group (such as $-CH_2-CH_2-$,[21,22,24,25] $-CH_2-$,[26] $-CH{=}CH-$,[22,23] or $-C_6H_4-$[24,27]), in addition to Si−O−Si linkages. Disordered materials (referred to as bridged silsesquioxanes) with such hybrid organosilica frameworks were reported in 1989[28] and have been actively studied because of their interesting properties, such as large specific surface areas and pore volumes, tailored framework properties, and surface functionality.[29,30] The bridged silsesquioxanes are often highly porous, but their porous structures are disordered and pore size distributions are broad. Therefore, the shaping of their porous structures using proper structure-directing agents, which is an essence of PMO synthesis,[21−23] is a highly promising new approach. PMOs are envisioned to have many remarkable properties related to the possibility of tailoring of their framework properties between those of ceramics and organic materials.[3,4] This tailoring can be achieved by selecting a suitable organic bridging group. Alternatively, a range of materials intermediate between pure organosilicas (with each silicon atom bonded to one carbon atom of the bridging organic group) and pure silicas can be obtained via co-condensation of organosilica precursors with silica precursors.[23,24] The resulting materials were indeed found to exhibit properties that systematically changed as the proportion of organosilica to silica components varied.[24] Surface properties of PMOs can also be tailored using the above two strategies (that is, the selection of the bridging organic group and the content of the organosilicate component), provided that the organic groups are actually exposed on the surface rather than buried in the framework. To this end, PMOs with $-CH{=}CH-$ bridges were reported to undergo reactions involving the organic group,[22,23] clearly demonstrating that these groups were actually accessible. In addition, wetting behavior[3,22] and low-pressure gas adsorption properties[31] indicated the exposure of $-CH{=}CH-$ and $-CH_2-CH_2-$ groups on the pore surface. Because of the presence of silanols in the structure of PMOs, it is additionally possible to modify the PMO surface via chemical bonding of organic groups.[24] The remarkable properties of PMOs make them attractive from the point of view of advanced nanostructured materials design.[3,4]

As-synthesized OMMs constitute another exciting group of OOINs.[5] They are known to be capable of undergoing phase transitions from one ordered phase to another,[32] and chemical reactions, such as those with organosilanes that were already discussed. Their composition (silica:surfactant molar ratio) under given synthesis conditions is often independent of the surfactant chain length or even surfactant structure.[33−35] In these composites, surfactant ions are located in the voids (pores) in the silicate framework.[5] The external surfaces of particles of these composites are also likely to be covered by a relatively dense layer of surfactant ions, as recently found for MCM-41 and MCM-48.[34,36,37] Because of the presence of surfactant, internal porous structures (that is surfactant-filled voids in the silicate framework) of as-synthesized OMMs were usually found largely or fully inaccessible to adsorbates, such as nitrogen.[34,36−38] Nonetheless, the ordered surfactant−silicate composites are capable of adsorbing nonpolar molecules from solutions[33,39] and catalyzing chemical reactions in the liquid phase.[40] This shows that the surfactant micelles confined in a periodic inorganic framework can effectively solubilize organics, which was also confirmed by the feasibility of expanding the size of voids in the silicate framework by swelling a preformed surfactant−silicate nanocomposite using neutral amines.[41]

Gas adsorption is commonly used in OOIN characterization,[2,6−10,12−15,19,21−25,27,31,34−38,40,42−63] allowing one to determine the specific surface area, pore volume, and pore size distribution as well as to study the surface properties. Many well-known adsorption methods for characterization of porous materials are applicable to OOINs,[51,64−68] but the custom-tailored structures of these materials create new challenges with respect to accuracy, reliability, and characterization capability and open new opportunities in the development of adsorption characterization methods. This review is intended to present the currently available gas adsorption methods suitable for characterization of OOINs. The discussion will cover the methodology of adsorption data analysis rather than adsorption data acquisition methodology, whose description can be found elsewhere.[64,65,68] First, it is discussed what types of adsorption isotherms and hysteresis loops are typically observed for OOINs and what structural information they provide as well

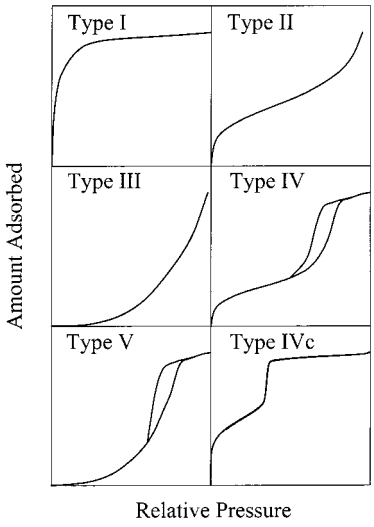

Figure 1. Classification of gas adsorption isotherms (after refs 65 and 68).

as what kind of information cannot be readily obtained from them on the basis of our current knowledge. Second, the methods for evaluation of the specific surface area and pore volume are presented with an emphasis on the issues specific for OOINs. Third, the approaches to evaluate the pore size and pore size distribution (PSD) are critically discussed, highlighting the recent developments related to the advances in the computational modeling of adsorption in porous media and to the application of OMMs as model adsorbents to test the existing methods for calculation of PSDs and to develop a novel, accurate, and reliable pore size analysis methodology. Finally, the opportunities in the characterization of the surface properties of OOINs using specific and nonspecific adsorbates are discussed with an emphasis on the detection of surface groups and the estimation of the surface coverage of organic ligands.

The Shape of a Gas Adsorption Isotherm as a Source of Qualitative Structural Information

Classification of Gas Adsorption Isotherms. Experimental gas adsorption isotherms usually fall into six categories,[65,68] out of which five (Types I−V according to the IUPAC classification,[65] see Figure 1) are relevant to the present discussion. Type I isotherms exhibit prominent adsorption at low relative pressures (the relative pressure is defined as the equilibrium vapor pressure divided by the saturation vapor pressure) and then level off. Type I isotherm is usually considered to be indicative of adsorption in micropores or monolayer adsorption due to strong adsorbent−adsorbate interactions (which may be the case for chemisorption, which involves chemical bonding between the adsorbate and the adsorbent surface; we will not discuss chemisorption here).[68] It should be noted that pores are classified herein on the basis of their diameter (or width) as micropores (below 2 nm), mesopores (between 2 and 50 nm), and macropores (above 50 nm).[65] In the case of nonpolar gases commonly used for characterization of porous solids (nitrogen, argon),[64−68] chemisorption is unlikely and therefore a classical interpretation would associate Type I with microporosity. However, Type I isotherms may also be observed for mesoporous materials with pore sizes close to the micropore range. In particular, in the case of adsorption of N_2 at 77 K or Ar at both 77 and 87 K in cylindrical pores, a Type I isotherm would have to level off below the relative pressure of about 0.1 for the material to be exclusively microporous, as inferred from the results of recent studies of siliceous OMMs.[35,69] Consequently, when a Type I isotherm does not level off below the relative pressure of 0.1, the sample is likely to exhibit an appreciable amount of mesopores or even be exclusively mesoporous. However, such Type I behavior may be indicative of some degree of broadening of the mesopore size distribution. This is because materials with highly uniform cylindrical pores may exhibit discernible steps on adsorption isotherms (and therefore these isotherms are classified as Type IV, as discussed later) at relative pressures down to 0.1 or perhaps even lower (for N_2 at 77 K and Ar at 77 and 87 K).[35,69] Type I isotherms are quite common for OMMs with organic groups bonded to a silica framework, both prepared via chemical bonding[47] and co-condensation.[19,54]

Adsorption on many macroporous solids proceeds via multilayer formation in such a manner that the amount adsorbed increases gradually as the relative pressure increases, although the multilayer buildup close to the saturation vapor pressure may be quite abrupt. This unrestricted multilayer formation process gives rise to Type II and III isotherms. In this case, the adsorption and desorption branches of the isotherm coincide; that is, there is no adsorption−desorption hysteresis. Depending on the surface properties of a given solid, there may be a pronounced stage of the monolayer formation (Type II) or the adsorption isotherm may be convex in the whole pressure range (Type III). The latter behavior can be observed when lateral interactions between adsorbed molecules are strong in comparison to interactions between the adsorbent surface and adsorbate. N_2 adsorption isotherms similar to Type II were reported for several as-synthesized (surfactant-containing) OMMs.[37,38] Type III adsorption isotherms were reported for water adsorption on certain OOINs with hydrophobic surfaces.[44,46,48,53]

Adsorption on mesoporous solids proceeds via multilayer adsorption followed by capillary condensation (Type IV and V isotherms). Therefore, the adsorption process is initially similar to that on macroporous solids, but at higher pressures the amount adsorbed rises very steeply due to the capillary condensation in mesopores. After these pores are filled, the adsorption isotherm levels off. Capillary condensation and capillary evaporation often do not take place at the same pressure, which leads to the appearance of hysteresis loops. However, it was suggested long ago[64] and unequivocally confirmed after the discovery of OMMs[70,71] that the capillary condensation−evaporation in mesopores may also be reversible (this behavior will be denoted herein as Type IVc).[68] Type IV in general, and IVc in particular, is typical for many OOINs with accessible mesopores, although when the size of the pores is close to the micropore range or PSD is broad, Type I isotherms can be observed. The distinction between Types IV and V is analogous to that between Types II and III. Finally,

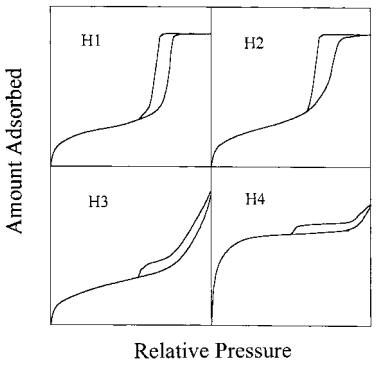

Figure 2. Classification of adsorption−desorption hysteresis loops (after ref 65).

it should be noted that some OOINs may exhibit adsorption isotherms that can be regarded as a combination of the aforementioned five types of isotherms as a result of the presence of several different types of pores in the structure.

Classification of Adsorption−Desorption Hysteresis Loops. As was already mentioned, the adsorption process on mesoporous solids is often accompanied by adsorption−desorption hysteresis. This phenomenon was a subject of numerous studies,[64,68,72−75] but its origin is still not fully understood. The hysteresis is usually attributed to the thermodynamic or network effects or the combination of these two effects.[68,72] The thermodynamic effects are related to the metastability of adsorption or desorption (or both) branches of the adsorption isotherm. Namely, the capillary condensation or evaporation may be delayed and take place at higher or lower pressures, respectively, in comparison to the pressure of coexistence between the gaslike and liquidlike phases in the pore. In addition, the hysteresis may also be caused by pore connectivity (network) effects, which are expected to play an important role in desorption processes. Namely, if larger pores have access to the surrounding only through narrower pores, the former cannot be emptied at the relative pressure corresponding to their capillary evaporation since the latter are still filled with the condensed adsorbate. So the larger pores may actually be emptied at the relative pressure corresponding to the capillary evaporation in the smaller connecting pores (or at the relative pressure corresponding to the lower limit of adsorption−desorption hysteresis). Hysteresis loops observed experimentally most likely arise from some combination of thermodynamic and network effects, although the latter are often particularly prominent. Adsorption isotherms for certain porous solids may also exhibit low-pressure hysteresis loops (loops that do not close, even at low relative pressures). Low-pressure hysteresis may arise from swelling of the adsorbent during the adsorption process or when physical adsorption is accompanied to some extent by chemisorption processes.[65]

According to the IUPAC recommendations,[65] hysteresis loops are classified into four types. The Type H1 loop exhibits parallel and nearly vertical branches (see Figure 2). This kind of hysteresis loop was often reported for materials that consisted of agglomerates (assemblages of rigidly joint particles) or compacts of approximately spherical particles arranged in a fairly uniform way.[65] More recently, it has become clear[68] that H1 hysteresis loops are also characteristic of materials with cylindrical pore geometry and a high degree of pore size uniformity.[32,76] Hence, the appearance of the H1 hysteresis loop on the adsorption isotherm for a porous solid generally indicates its relatively high pore size uniformity and facile pore connectivity. The Type H2 hysteresis loop has a triangular shape and a steep desorption branch. Such behavior was observed for many porous inorganic oxides and was attributed to the pore connectivity effects,[74] which were often considered to be a result of the presence of pores with narrow mouths (ink-bottle pores), but the latter identification may be grossly oversimplified. Indeed, H2 hysteresis loops were observed for materials with relatively uniform channel-like pores, when the desorption branch happened to be located at relative pressures in the proximity of a lower pressure limit of adsorption−desorption hysteresis.[76] This lower limit is characteristic of a given adsorbate at a given temperature (a relative pressure of about 0.4 for N_2 at 77 K; 0.34 and 0.26 for Ar at 87 and 77 K, respectively). It should be noted that, in certain relatively rare cases, hysteresis extends below this limit; that is, low-pressure hysteresis is observed. Thus, the appearance of a H2 hysteresis loop in the proximity of the lower pressure limit of adsorption−desorption hysteresis should not be regarded as evidence of poor pore connectivity or ink-bottle pore shape. In fact, novel materials having uniform cagelike pores (and thus suitable as model solids with ink-bottle pores) exhibited adsorption isotherms with broad hysteresis loops but without any dramatic differences in steepness of adsorption and desorption branches.[77−79] These hysteresis loops seemed to be intermediate between Types H2 and H1, rather than being Type H2, as could be expected from the aforementioned simplistic interpretation.

Isotherms with Type H3 loops that do not level off at relative pressures close to the saturation vapor pressure were reported for materials comprised of aggregates (loose assemblages) of platelike particles forming slitlike pores. Type H4 loops feature parallel and almost horizontal branches and their occurrence has been attributed to adsorption−desorption in narrow slitlike pores. However, recent experimental data for well-defined systems question this interpretation. Namely, the Type H4 loop was reported for MCM-41 that exhibited particles with internal voids of irregular shape and broad size distribution (between 5 and 30 nm).[80] Hollow spheres with walls composed of ordered mesoporous silica also exhibited hysteresis behavior of the H4 type.[81] This would suggest that H4 hysteresis loops may merely arise from the presence of large mesopores embedded in a matrix with pores of much smaller size. Because Type H3 loops are quite similar to Type H4 loops, one can also expect that the former are not attributable solely to platelike materials with slitlike pores. It should be noted that an appearance of a hysteresis loop similar to Type H4 but of triangular shape with an almost horizontal desorption branch that falls steeply close to the lower limit of adsorption−desorption hysteresis may be indicative of the presence of disordered domains resulting from collapse of lamellar structures.[82]

Determination of Specific Surface Area and Pore Volume

Specific Surface Area. Currently, there are two major methods used to evaluate specific surface area from gas adsorption data: the Brunauer−Emmett−Teller (BET) method[64−68,83] and the comparative method.[64,68] The evaluation of the specific surface area using the BET method is based on the evaluation of the monolayer capacity (that is, the number of adsorbed molecules in the monolayer on the surface of a material) by fitting experimental gas adsorption data to the BET equation. Thus, obtained monolayer capacity is multiplied by the cross-sectional area of the adsorbed molecule in the monolayer formed on a given surface. The comparative method is based on the comparison of the adsorption isotherm for a given porous material with the adsorption isotherm for a suitable reference adsorbent of known specific surface area.

The derivation of the BET equation involves the following major assumptions: the surface is flat; all adsorption sites exhibit the same adsorption energy; there are no lateral interactions between adsorbed molecules; the adsorption energy for all molecules except for the first layer is equal to the liquefaction energy; and an infinite number of layers can form. In the case of adsorption on actual porous solids, these assumptions usually do not hold. In particular, surfaces are geometrically and energetically heterogeneous, there are lateral interactions between adsorbed molecules, and interactions of adsorbed molecules vary with the distance from the surface.[64,66,68] Therefore, one should not expect the monolayer capacity derived using the BET method to be particularly accurate. In addition, the values of cross-sectional areas (denoted as ω) of adsorbed molecules, even those most commonly used, are currently somewhat uncertain and may actually vary from one type of surface to another. [64,68,84,85] Moreover, the very concept of determination of the specific surface area on the basis of molecular size and monolayer capacity should be treated with some caution because the ability of molecules to effectively cover the surface is dependent on the molecular size and surface corrugation.[68,86] Clearly, adsorbed molecules cannot satisfactorily probe surface roughness on the scale smaller than their size. Therefore, the surface areas determined using larger molecules may be smaller than those obtained using smaller molecules. Because one usually employs small N_2 molecules or Ar atoms to evaluate the specific surface area, the aforementioned problems with the inadequate probing of the surface roughness are not expected to be severe for many OOINs. However, for OOINs with fairly large organic surface groups that do not form compact layers, the surface may be highly rough and difficult to probe adequately by any kind of adsorbate, and even the very concept of the surface may be somewhat ill-defined. In addition, one needs to keep in mind that the value of the monolayer capacity multiplied by the cross-sectional area of adsorbed molecules essentially provides the area of the surface drawn through the centers of adsorbed molecules, which may be different from the geometrical surface area of the solid. For instance, in the case of approximately cylindrical pores, the underestimation of the geometric specific surface area would be by the factor of about $w/(w - \sigma)$, where w is the pore diameter and σ is the diameter of the adsorbed molecule. In the case of nitrogen adsorption, this factor is more than 10% for typical OOINs with cylindrical pores of diameter below 4 nm.

Despite all these problems and limitations, the BET method is currently a standard in the specific surface area evaluation,[68] perhaps largely because other methods, except for the comparative analysis that is described below, do not offer any appreciable advantages, and at the same time their limitations are less well-understood, and these methods themselves may be more difficult to apply. Moreover, even the assessment of the specific surface area using the comparative method often employs data for reference samples for which the specific surface area was evaluated using the BET method. Because the BET method is so commonly used and it is often unclear what alternative approaches can be used to substitute it, it is worthwhile to discuss how to use this method effectively for OOINs. The discussion will be focused on the application of N_2 and Ar adsorption because these gases are most commonly used in the BET analysis.[68]

In general, it is recommended to use adsorption data at relative pressures below 0.3 in N_2 BET calculations.[67] However, even in this case the results will depend to some extent, sometimes considerably, on the choice of the relative pressure interval used.[87] This needs to be taken into account when the specific surface areas for different samples are compared. It is advised to report the relative pressure range used along with the results of the BET calculations.[65,68] Moreover, it is often advised to establish a relative pressure range where the BET equation provides the best description of the experimental data and then to use this range to determine the BET monolayer capacity for a given sample. Because a selection of such a range is often largely arbitrary and the use of different ranges for different samples may make the comparison of their specific surface areas difficult, we do not recommend this practice. Instead, we suggest using the same range of relative pressures for a given adsorbate and type of adsorbents, if only this procedure is practical and applicable (some criteria of applicability of a given relative pressure range that are relevant to OOINs characterization are discussed later). This would not only help in comparative studies, but would also permit the evaluation of the accuracy of calculations using model adsorbents, whose specific surface areas can be evaluated independently with reasonable accuracy. These model adsorbents currently include uniform spherical nonporous particles[84] and OMMs (including OOINs), whose specific surface areas can be determined, respectively, using electron microscopy data and using the combination of data from two or three different experimental techniques, including powder X-ray diffraction (XRD).[52,69,76] The studies of uniform spheres by Jelinek and Kovats provided convincing evidence that N_2 BET specific surface area evaluated from data in the relative pressure range from 0.05 to 0.23 is in agreement with the geometrical surface area when the cross-sectional area (ω) for N_2 on silica was 0.135 nm^2, and was 0.168 nm^2 for nitrogen on the silica surface fully covered with a dense layer of ligands with long alkyl chains.[84] The latter ω value is close to

the commonly accepted one (0.162 nm^2),[65,67] but ω suggested for silica is quite low. Although it is not improbable that the N_2 molecule can orient on the silica surface in such a way that $\omega = 0.135$ nm^2 can be attained, there is another possible interpretation of the data of Jelinek and Kovats. Namely, the validity of the derived cross-sectional areas rested upon an assumption that the values of the BET monolayer capacity determined in the pressure range used were correct. However, there is evidence that suggests that the monolayer capacity evaluated for silica is overly large when the considered relative pressure range is used in the BET analysis, and consequently $\omega = 0.135$ nm^2 was an underestimation of the actual value. The evidence was obtained from studies of adsorption in uniform MCM-41 pores, whose size was evaluated using independent methods.[88,89] The well-defined pore geometry of MCM-41 allowed for a reliable calculation of the statistical film thickness of adsorbate in the pores,[76] to find out at which relative pressure the thickness corresponding to the statistical monolayer is attained, and consequently to determine the monolayer capacity as the amount adsorbed corresponding to this relative pressure.[52] It was found that the statistical film thickness of nitrogen in silica pores is much larger than that usually assumed, and as a result the monolayer capacity is much smaller than that resulting from the BET analysis in the relative pressure intervals typically used. The magnitude of the monolayer capacity overestimation for N_2 adsorption on silicas is quite similar to the ratio of the standard N_2 cross-sectional area to the cross-sectional area determined by Jelinek and Kovats.[84] Therefore, the deviations of their results from the commonly accepted value of ω for N_2 on the silica surface might have merely resulted from the inability of the BET method to provide the correct monolayer capacity. This argument is based on the assumption that the commonly used monolayer statistical film thickness for N_2 (0.354 nm)[68] is valid for the silica surface. If N_2 molecules actually exhibit orientation effects, this assumption may be invalid. Anyway, it is clear that, without additional data from other experimental techniques, the conclusion of Jelinek and Kovats about ω of nitrogen on silicas appears premature and this is probably not ω, but the calculation of the monolayer capacity that should be corrected. The latter correction can actually be achieved by changing the pressure range used in the BET calculations because this range has a prominent effect on the results in the case of silicas.[87] However, from the practical point of view, the relative pressure range for the BET calculations and the corresponding ω determined by Jelinek and Kovats can be used to obtain an accurate assessment of the specific surface area for silicas, if only other conditions required for the applicability of the BET equation are fulfilled in this relative pressure range. These conditions will be discussed below. Although the use of MCM-41 as a model adsorbent suggested that the results of Jelinek and Kovats for silicas should be reinterpreted, the use of OOINs as model adsorbents provided a confirmation of their results for strongly hydrophobic surfaces. In this case, the BET analysis in the relative pressure range from 0.05 to 0.23 appears to provide a generally correct estimate of the monolayer capacity.[52]

These findings are directly relevant to the specific surface area determination for OOINs. In the case of such materials with surfaces that interact with nitrogen or argon similarly to the silica surface (for instance, siliceous OMM with chemically bonded polymeric aminopropyl ligands),[45] the monolayer capacity calculated using the BET method in the relative pressure range similar to that used by Jelinek and Kovats will be most likely overestimated. To compensate for the resulting error, one can use a lower value of ω, such as 0.135 nm^2, keeping in mind that this value does not have an actual physical significance. Alternatively, the pressure range used for the BET analysis for silicas will need to be modified[52] or an empirical correction to compensate for the error from the determination of the monolayer capacity using the BET method for silicas in the typical relative pressure range can be introduced. In the case of OOINs with strongly hydrophobic surfaces, such as those covered by dense layers of long alkyl chains, the BET monolayer capacity calculated in a typical relative pressure range (such as 0.05−0.23) is likely to be correct and an accurate estimate of the specific surface area can be derived from it using the cross-sectional area commonly used for N_2 (that is, 0.162 nm^2). The studies of Ar adsorption at 87 K on siliceous OMMs and OOINs indicate that the BET monolayer capacity obtained in the relative pressure range similar to the above is rather accurate, and reasonable values of the specific surface area can be obtained when $\omega = 0.138$ nm^2 is used.[69] In all cases, one needs to keep in mind that the derived specific surface area may actually reflect the area of the surface drawn through centers of adsorbed molecules, and therefore it may be appropriate to introduce a suitable correction for the pore shape, as discussed above. In many routine studies, the introduction of the aforementioned corrections may not be necessary, although the approximate nature of thus obtained specific surface area estimates should be kept in mind.

In addition, one needs to restrict the BET calculations to a range of gas adsorption data wherein the assumptions of the method are most closely fulfilled, if only such a range can be found. This is an important problem in the case of OOINs, whose adsorption isotherms are often either of Type IVc with the capillary condensation step below the relative pressure of 0.3, or Type I. In these cases, the adsorption in the relative pressure range potentially usable for the BET analysis does not proceed exclusively as a multilayer formation, as the BET equation assumes, but has contribution from capillary condensation or micropore filling phenomena or both of the above. It is clear that the data from the capillary condensation or micropore filling regions as well as from the plateau observed after the pores have been filled should not be used, if possible, in the BET analysis. So in the case of the Type IVc isotherm, one is forced to select the data at relative pressures below the onset of capillary condensation. For the Type I isotherm, there might be no range of data points, where adsorption would proceed in a way close to unrestricted multilayer formation, and perhaps the best choice is to use data somewhere below the relative pressure at which the isotherm levels off. Obviously, the resulting BET monolayer capacity will need to be treated with caution.[68] It can be concluded that, despite its limitations and

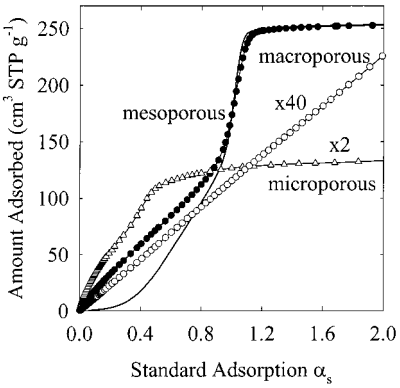

Figure 3. Comparative plots calculated for a microporous (as-synthesized ethanol-washed C12 MCM-41),[36] mesoporous (ODMS-modified MCM-41),[52] and macroporous (ODMS-modified silica)[52] hydrophobic adsorbents using reference data for macroporous ODMS-modified silica. The solid line without symbols shows the comparative plot for the hydrophobic mesoporous adsorbent calculated using the reference data for silica. Data partially taken from ref 52.

shortcomings, the days of the BET analysis are not over. The method can still provide useful information about the specific surface area, although some caution should be taken to select a proper range of data for the calculations and use appropriate values of the molecular cross-sectional areas. When an accurate determination of the geometrical specific surface area is required, one can introduce suitable corrections for the pore shape. Finally, it needs to be kept in mind that even when these precautionary measures are taken, the BET specific surface areas derived from Types II and IV isotherms may still be somewhat inaccurate, although perhaps closer than within 20% (which was provided as an estimate of accuracy of the BET monolayer capacity in the well-known monograph; ref 64, p 61) of the actual value. However, lower accuracy can be expected for isotherms of Types I, III, and V, but fortunately these last two types are not common in the case of the specific surface area evaluation for OOINs using N_2 or Ar.

After the many problems associated with the BET analysis were considered, the concept of the comparative analysis of adsorption data can be readily appreciated. The comparative analysis is based on the idea of comparing the adsorption isotherm for material under study with the adsorption isotherm of a reference macroporous solid of the same surface properties with respect to the adsorbate used. The adsorption on the macroporous reference solid proceeds as multilayer adsorption essentially in the entire relative pressure range, except perhaps the relative pressures very close to the saturation vapor pressure, where capillary condensation may also be observed. If the compared solid is also macroporous, the adsorption on its surface also proceeds via multilayer formation. When the amount adsorbed on the compared solid is plotted as a function of the amount adsorbed on the reference adsorbent at the same relative pressure values, a straight line is observed because the amount adsorbed on one of these solids is proportional to the other, whereas the proportionality constant is simply the ratio of the specific surface areas of these two solids. This situation is depicted in Figure 3 for two macroporous silicas modified with octyldimethylsilyl (ODMS) ligands. One of these adsorbents was chosen as a reference (for the latter, the amount adsorbed is expressed as standard reduced adsorption, α_s, which will be defined below). So if the specific surface area of the reference solid is known, the specific surface area of the compared solid can readily be determined from the comparative plot. This is advantageous because once an accurate surface area evaluation is achieved for the reference solid, the specific surface area of the compared material can be accurately evaluated from adsorption data in essentially any relative pressure range. The analysis along the lines described above can be carried out for both Types II and III isotherms. Initial parts of Types IV and V isotherms (that is, the parts at relative pressures below the onset of capillary condensation) also provide straight lines when an appropriate reference adsorbent is used (see Figure 3). This allows one to assess the specific surface area. Moreover, the slope of a linear segment of the comparative plot at relative pressures where the mesopores are already filled with condensed adsorbate provides an estimate of the external surface area of the material, whereas the intercept of the line passing through this segment with the "Amount Adsorbed" axis of the plot reflects the adsorption capacity of mesopores. This quantity can be recalculated to the corresponding volume of mesopores (see below). In the case of Type I isotherms, the external surface area and the micropore and/or mesopore volume can be determined in the same manner. However, because adsorption in pores of size within or close to micropore range is enhanced at low relative pressures, the slope of the initial part of the comparative plot for the Type I isotherm will in general be higher than that corresponding to the specific surface area. Therefore, the resulting specific surface area estimates for Type I isotherms should be treated with caution, especially when the compared material is largely or exclusively microporous.

This discussion was based on an assumption that the reference solid exhibits the surface properties very similar to those of the compared solid in the case of the adsorbate used. If this is not the case, the comparative plot analysis becomes more complicated. The differences in surface properties may cause various deviations of the comparative plot from linearity. These deviations themselves can be analyzed to gain some useful inferences about the nature of the surface of the compared.[51,90,91] To obtain good estimates of the specific surface area, especially from Types IV and V isotherms, is necessary to have a reference adsorbent whose surface properties are as close as possible to those of the compared solid so as to eliminate the aforementioned deviations. This is illustrated in Figure 3, where the comparative plots for OOIN with a highly hydrophobic surface were obtained using the reference adsorbents of a similar surface nature and largely different surface nature. When the appropriate reference adsorbent was employed, the initial part of the plot was approximately linear and could be used to determine the specific surface area, whereas in the other case, such determination was impossible because the comparative plot was strongly bent downward. In both cases, the mesopore volume and the external surface area could be determined and were acceptably close, which reflects the well-known observation that surface properties affect

the low-pressure part of the adsorption isotherm more strongly than the multilayer adsorption part at higher relative pressures.

The comparative analysis is very useful in characterization of adsorbents. However, the number of reference adsorption isotherms currently available in the literature is limited and, as far as we know, only one of them was reported in a tabular form for a material with an organic-modified surface (that is, for strongly hydrophobic ODMS-modified silica).[52] Therefore, there seem to be currently only two choices of reference data relevant for OOINs, one being the data for silica[64,87] and the other one being the data for the aforementioned modified material.[52] Unfortunately, in none of these cases was an estimate of the specific surface area made independent from the BET analysis, although in both cases the accuracy of the BET specific surface area was generally assessed[52] and thus fairly accurate estimates of the actual specific surface area can be established. It would be desirable to acquire the reference adsorption isotherms for various types of surfaces encountered in cases of OOINs. Finally, it should be mentioned that there are several different versions of the comparative analysis, which are essentially equivalent, but differ in ways of expressing amounts adsorbed on the reference solid, or on both the reference solid and the compared solid. In the t-plot method,[64] the amount adsorbed for the reference is expressed as the statistical film thickness curve (t-curve). However, the determination of the t-curve usually requires knowledge of the specific surface area, which is often not known with satisfactory accuracy.[92] Therefore, it was suggested to be more convenient to express the amount adsorbed for the reference adsorbent as the standard reduced adsorption, that is, the amount adsorbed (as a function of pressure) divided by the amount adsorbed at an arbitrarily chosen relative pressure (usually 0.4).[64,68] This modification of the comparative plot method is referred to as the α_s plot method and is perhaps the most popular today. Other legitimate choices can also be made in the expression of the amount adsorbed for the reference adsorbent.[90,91]

Pore Volume Determination. The total pore volume of a given adsorbent can be calculated from the amount adsorbed at a relative pressure close to the saturation vapor pressure (for instance, at a relative pressure of 0.99) simply by converting this amount adsorbed to the corresponding volume of liquid adsorbate at the temperature of the adsorption measurement. In the case of N_2 at 77 K and Ar at 87 K, the conversion factors from the amount adsorbed (expressed in cm^3 STP g^{-1}; STP stands for standard temperature and pressure) to the volume of liquid adsorbate are 0.0015468 and 0.001279,[69] respectively, under the assumption that the density of condensed adsorbate in the pores is equal to the density of bulk liquid adsorbate. This assumption appears to be satisfactory for mesopores. The total pore volume determined as described above reflects the volume of all pores in which the capillary condensation and micropore filling have taken place plus the volume of adsorbed film on the surface of the pores in which the capillary condensation did not take place. The determination of the mesopore volume and micropore volume using the comparative method was discussed above. In the case of the two OOIN samples whose comparative plots are presented in Figure 3, these calculations provide the volume of ordered pores. The latter are often referred to as primary pores, to distinguish them from disordered, for instance, interparticle, mesopores and macropores of the size below about 200−400 nm that are often referred to as secondary (textural) pores. It should be noted that the range for pores in which capillary condensation takes place at relative pressures distinguishable from the saturation vapor pressure varies from one adsorbate to another and it is additionally dependent on temperature. For instance, the upper limit of this range is similar for N_2 at 77 K and Ar at 87 K and appears to be about 200−400 nm, whereas it is only about 20 nm for Ar at 77 K.

For some adsorbents, the pore volume simply cannot be correctly determined using a given adsorbate because the pores are not fully filled with the adsorbate at any relative pressure discernible from the saturation vapor pressure. For instance, this is the case for water adsorption on hydrophobic surfaces of certain OOINs because the hydrophobic surface groups hinder the formation of multilayer (or clusters) of water.[44,46,48,53] Another example is provided by benzene adsorption on OOINs with phenyl groups on the surface. The presence of the latter apparently prevents the adsorbed molecules from accessing a part of otherwise available pore volume, probably because of the steric hindrance.[55] Therefore, it is often beneficial to use small molecules, such as N_2 or Ar, that can more readily probe the accessible pore volume of OOINs.

Determination of Pore Size and Pore Size Distribution

Pore Diameter. The structural properties of OOINs with accessible ordered porosity are expected to fulfill certain geometrical relations arising from the uniform ordered nature of the pores. In the case of materials with uniform cylindrical pores, the diameter of ordered pores, w, is related to their volume, V_p, and geometrical surface area, S, through the following simple equation: $w = 4V_p/S$,[70] which was employed in some studies of OOINs.[24,42] Although both V_p and S are available from gas adsorption data, this relation for the pore diameter is not as useful as it seems to be because of the uncertainty in the determination of the geometrical surface area using the available methods. Therefore, one should search for relations that involve parameters that can be determined with satisfactory accuracy, providing a reliable method for the pore diameter evaluation for OOINs. A very useful relation involves the pore diameter, pore volume, and (100) interplanar spacing, d_{100}, for 2-D hexagonal structures similar to that of MCM-41:[88,89]

$$w = cd_{100}\left(\frac{V_p\rho}{1 + V_p\rho}\right)^{1/2} \quad (1)$$

where ρ is the density of pore walls of the material and c is a constant characteristic of the pore geometry and equal to 1.213 for cylindrical pores. The (100) interplanar spacing can be evaluated using XRD or transmission electron microscopy. Equation 1 was employed in pore diameter calculations for a variety of OMMs, including MCM-41 silica,[69,76,89,93−95] non-silica porous oxides,[94] and

PMOs.[31] The results for different samples of the same composition[69,76] as well as for samples with different compositions[31] are remarkably consistent despite the fact that, in most cases, the pore wall density used in calculations was estimated from the literature data rather than measured. Unfortunately, PMOs are the only group of OOINs for which eq 1 is directly applicable. In the case of OOINs with silica frameworks and organic ligands on the surface, one can attempt to introduce the density of organic groups to the calculations, as was proposed in ref 63 without providing the actual calculation procedure. For OOINs obtained via postsynthesis surface modification of MCM-41 or similarly structured materials, an equation was derived to determine the pore size from the ratio of pore volumes before and after modification, the pore size of unmodified material, and the weight percentage of the organic moieties introduced.[45] This simple equation was employed in the pore diameter calculation for OOINs used as model adsorbents to determine the reference t-curve of N_2 on the organic-modified silica.

Pore Size Distribution. There are many methods for calculation of pore size distributions (PSDs),[64,66,68] and most of them are potentially applicable for OOINs. However, the ordered nature of OOINs and the tendency to custom-tailor their structures impose stringent requirements on the accuracy and reliability of the methods for the PSD calculation. Unfortunately, many of the available methods do not fulfill these criteria because either they do not allow one to assess the pore size with acceptable accuracy or they produce artifacts, which would be potentially misleading. PSDs for OOINs are usually evaluated using methods based on either the Kelvin equation[96−102] or the Horvath−Kawazoe method[103] and its modifications.[104] The first group includes the methods of Barrett, Joyner, and Halenda (BJH),[96] Cranston and Inkley (CI),[97] Dollimore and Heal (DH),[98] and Broekhoff and de Boer (BdB).[99−102] The BJH method was commonly used in OOINs characterization.[21,22,25,38,44,49,53,57]Although the BJH, CI, and DH methods are often considered as appreciably different, all of them are based on the general concept of an algorithm outlined in the BJH work,[96] although the latter originally suggested a simplification that was later eliminated in the CI and DH approaches. To implement the algorithms proposed in these three methods, the knowledge of a relation between the pore size and capillary condensation or evaporation pressure and the t-curve is required, and a choice needs to be made as to which branch of the isotherm is appropriate for PSD calculations. The original BJH, CI, and DH works are not fully consistent as far as the selection of these relations and the choice of the branch of the isotherm are concerned. These inconsistencies are capable of affecting the results of calculations much more than the minor differences in the algorithms,[105] being most likely responsible for claims that these three methods appreciably differ.

The BJH, CI, and DH methods assume the same general picture of the adsorption−desorption process. Adsorption in mesopores of a given size is pictured as multilayer adsorption followed by capillary condensation (filling of the pore core, that is, the space that is unoccupied by the multilayer film on the pore walls) at a relative pressure determined by the pore diameter. The desorption is pictured as capillary evaporation (emptying of the pore core with retention of the multilayer film) at a relative pressure related to the pore diameter, followed by thinning of the multilayer. It has recently been confirmed using MCM-41 with approximately cylindrical pore geometry (that is assumed in the BJH, CI, and DH algorithms) that this general picture reflects the actual nature of adsorption in mesopores.[69,76] These methods also adopted the concept of a common t-curve for mesopores of different sizes. This has also been tested using MCM-41 and found to be acceptably accurate,[35,36,69,76] although some increase in the statistical film thickness was observed as the pore size approached the micropore range. The BdB method, which is from the computation point of view an extension of the BJH, CI, and DH methods, attempted to account for the differences in the statistical film thickness in pores of different size. The aforementioned model studies indicate that this type of correction is generally beneficial, although certainly not crucial.

Because the concept underlying the BJH, CI, and DH algorithms appears to be correct, it is important to (i) establish an accurate relation between the pore size and capillary condensation or evaporation pressure, (ii) determine the correct t-curve (or a set of t-curves), and (iii) verify whether adsorption or desorption, or both branches of the isotherms, are suitable for the accurate pore size assessment. This would allow one to perform accurate PSD calculations using these simple algorithms. To this end, theoretical considerations,[64] nonlocal density functional theory (NL DFT) calculations,[75,106] computer simulations,[107] and studies of model adsorbents[69,76] strongly suggested that the Kelvin equation commonly used to provide a relation between the capillary condensation or evaporation pressure and the pore size underestimates the pore size. The DFT calculations,[75,108] computer simulations,[107] and novel methods based on the use of OMMs as model adsorbents[69,76] provided consistent results for N_2 at 77 K in cylindrical pores having diameters from about 2.5 to 4.0 nm. This range is particularly important from the point of view of OMM and OOIN characterization because it covers the typical pore sizes of these materials. The relations (determined using OMMs[69,76] and OOINs[52] as model adsorbents) between the pore diameter and the capillary condensation pressure for N_2 at 77 K and Ar at 87 K in silica and hydrophobic (ODMS-modified) pores are provided in Table 1.

Unfortunately, for larger pore sizes, the results derived on the basis of DFT data[75,108] and those obtained using model OMM materials diverged (the data from computer simulations[107] did not extend beyond $w = 5$ nm, so comparison could not be made). This divergence is likely to be related to the fact that it is difficult to unequivocally assign the branches of hysteresis loops and the equilibrium transition point from DFT calculations to the experimentally measured adsorption and desorption branches of isotherms. Indeed, two versions of the DFT-based procedures to calculate PSDs provide consistent results at relative pressures where hysteresis is not observed experimentally and thus the equilibrium transition point can be unequivocally assigned to the position of both these branches. However, in the hys-

Table 1. Values of the Capillary Condensation Pressure (p/p_0) and the Corresponding Pore Diameters (w) in Nanometers for Nitrogen on the Silica and ODMS-Modified Surfaces at 77 K and Argon on the Silica Surface at 87 K[52,69,76]

p/p_0	$w_{silica}(N_2)$	$w_{ODMS}(N_2)$	$w_{silica}(Ar)$	p/p_0	$w_{silica}(N_2)$	$w_{ODMS}(N_2)$	$w_{silica}(Ar)$
0.05	2.08	1.70	1.92	0.43	4.36	4.16	4.08
0.06	2.15	1.79	1.99	0.44	4.44	4.24	4.16
0.07	2.22	1.86	2.06	0.45	4.52	4.32	4.23
0.08	2.28	1.94	2.12	0.46	4.60	4.41	4.31
0.09	2.34	2.01	2.18	0.47	4.69	4.50	4.39
0.10	2.40	2.07	2.24	0.48	4.78	4.59	4.47
0.11	2.46	2.14	2.30	0.49	4.87	4.68	4.55
0.12	2.51	2.20	2.35	0.50	4.96	4.78	4.64
0.13	2.57	2.26	2.41	0.51	5.06	4.88	4.73
0.14	2.62	2.32	2.46	0.52	5.16	4.98	4.82
0.15	2.68	2.38	2.51	0.53	5.27	5.09	4.92
0.16	2.73	2.43	2.56	0.54	5.38	5.20	5.02
0.17	2.78	2.49	2.61	0.55	5.49	5.32	5.12
0.18	2.83	2.55	2.66	0.56	5.61	5.44	5.23
0.19	2.89	2.61	2.71	0.57	5.73	5.56	5.34
0.20	2.94	2.66	2.76	0.58	5.86	5.69	5.46
0.21	2.99	2.72	2.81	0.59	5.99	5.83	5.58
0.22	3.04	2.78	2.86	0.60	6.13	5.97	5.70
0.23	3.10	2.83	2.91	0.61	6.28	6.12	5.84
0.24	3.15	2.89	2.96	0.62	6.43	6.27	5.97
0.25	3.21	2.95	3.02	0.63	6.59	6.43	6.12
0.26	3.26	3.01	3.07	0.64	6.75	6.60	6.27
0.27	3.32	3.07	3.12	0.65	6.93	6.78	6.43
0.28	3.37	3.13	3.17	0.66	7.12	6.97	6.60
0.29	3.43	3.19	3.23	0.67	7.31	7.17	6.78
0.30	3.49	3.25	3.28	0.68	7.52	7.38	6.97
0.31	3.55	3.31	3.33	0.69	7.74	7.60	7.17
0.32	3.61	3.37	3.39	0.70	7.97	7.83	7.38
0.33	3.67	3.44	3.45	0.71	8.22	8.08	7.60
0.34	3.73	3.50	3.51	0.72	8.48	8.35	7.84
0.35	3.79	3.57	3.56	0.73	8.77	8.64	8.10
0.36	3.86	3.64	3.62	0.74	9.07	8.94	8.38
0.37	3.93	3.71	3.69	0.75	9.39	9.27	8.67
0.38	3.99	3.78	3.75	0.76	9.74	9.62	8.99
0.39	4.06	3.85	3.81	0.77	10.12	10.01	9.34
0.40	4.13	3.93	3.88	0.78	10.54	10.42	9.71
0.41	4.21	4.00	3.94	0.79	10.99	10.88	10.12
0.42	4.28	4.08	4.01	0.80	11.48	11.37	10.57

teresis region, this assignment needs to be modified because adsorption and desorption branches do not coincide. In principle, the experimental desorption branch should correspond to a certain point between the DFT desorption branch and the equilibrium transition point, whereas the experimental adsorption branch should correspond to a certain point between the equilibrium transition point and the metastable desorption branch determined from DFT. Clearly, different legitimate assignments can be made consistent with the above identification. Similar problems are encountered in the case of computer simulations of adsorption. It is thus not surprising that the two current DFT-based procedures to calculate PSDs for cylindrical pores from N_2 data at 77 K provide significantly different pore size estimates in the hysteresis region. For instance, for the same MCM-41 sample whose pore size was estimated as 5.5 nm using eq 1,[76] one of the DFT-based procedures[75,109] provided a pore diameter of 5.1 nm,[110] whereas the other one[108] suggested 6.0 nm. This indicates that the assignment of the DFT predictions to experimental hysteresis loops needs to be clarified before procedures to calculate PSDs using the DFT-based data can be regarded as fully reliable for materials whose isotherms exhibit pronounced hysteresis.

Because the reliability of advanced computational methods to calculate PSDs is yet to be improved, it is suggested to perform PSD calculations for OOINs using the BJH, CI, or DH algorithms. In doing so, adsorption rather than desorption data should be employed to avoid artifacts and to improve accuracy of the pore size determination. It was already discussed herein that desorption is often delayed because of network effects.[64,68,72−74] Surprisingly, the delayed desorption can even be observed for MCM-41, which is one of the most highly ordered mesoporous materials currently known. This effect probably arises from nonuniformity in diameter along the MCM-41 pores, which causes a situation where wider pore parts cannot be emptied until narrower pore parts separating them from the surrounding area are emptied or the relative pressure approaches the lower limit of adsorption−desorption hysteresis.[111] Spectacular effects of delayed capillary evaporation are observed for Type H4 hysteresis loops, where desorption can be observed at much lower pressures than those attributable to the actual pore sizes.[80,81] Therefore, we suggest avoiding use of desorption data in the pore size analysis. It should be noted that the combined analysis of both branches of adsorption isotherms may provide valuable insights into the connectivity[74] and size of constrictions in the porous structure.[58,112] However, recent studies of highly ordered MCM-41[36,111] suggest that our current knowledge of the desorption behavior in uniform pores is far from being

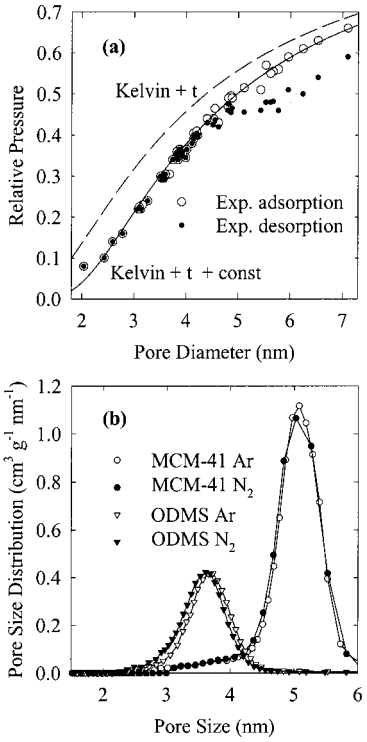

Figure 4. (a) The experimental relations between the MCM-41 pore diameter and capillary condensation (experimental adsorption) relative pressure as well as capillary evaporation (experimental desorption) relative pressure. The dashed line shows predictions of the Kelvin equation with the statistical film thickness correction, whereas the solid line shows the relation between the pore size and the capillary condensation pressure (the Kelvin equation with t-curve correction and additional correction) proposed in ref 76. Data partially taken from refs 36 and 76. (b) Pore size distributions for MCM-41 and ODMS-modified MCM-41 calculated from N_2 data at 77 K and Ar data at 87 K using the BJH method calibrated using MCM-41 and OOINs.[52,62,69,76] Data taken from ref 62.

satisfactory, and thus it may be very difficult to develop a reliable methodology for this kind of structural characterization.

Relations between the pore size and the capillary condensation pressure suitable for the BJH, CI, and DH calculations have recently been established for N_2 at 77 K and Ar at 87 K using MCM-41 silicas with pore sizes from about 2 to 6.5 nm.[69,76] These relations were reported in the form of empirical equations extrapolated over the entire mesopore range, and the agreement of one of them with the experimental data (determined using eq 1) for more than 60 MCM-41 samples is shown in Figure 4a. It would be desirable to test the validity of the extrapolation beyond the pore size range attainable for good-quality MCM-41, but this is currently difficult because of the problems in finding model extra-large-pore materials (SBA-15 silica[113] that was the most promising of them has been shown to have small connecting pores in the pore walls of large uniform pores).[61] Finally, the application of the BJH, CI, and DH approaches requires the availability of proper t-curves. The t-curves for N_2 at 77 K and Ar at 87 K adsorption on silica[69,87] and the t-curve for N_2 adsorption at 77 K on the surface of ODMS-modified silica were reported.[52] All of these t-curves are highly useful in the characterization of OOINs.[13,31,45,50−52,59−62] As can be seen in Figure 4b, PSD calculations provided remarkably consistent results for N_2 at 77 K and Ar at 87 K when the BJH-based algorithm with proper relations between the pore size and capillary condensation pressure and suitable t-curves were used, and calculations were based on adsorption rather than desorption data.[62] However, there is a need to derive t-curves for some other types of OOIN surfaces. To this end, a suitable procedure was outlined in ref 52 and should be helpful in this endeavor.

Some comments need to be made about the BdB and HK methods that have recently become increasingly popular. The BdB method[99−102] constitutes a major improvement over the BJH, CI, and DH methods in their original form.[96−98] However, one can readily verify that the predictions of the BdB method[100,102] are inconsistent with the data on OMMs (Table 1). Because of its rather complicated nature, it is not clear how the BdB method can benefit from the calibration using OMMs. In contrast, the BJH, CI, and DH approaches allow for easy introduction of appropriate corrections. Consequently, the application of proper t-curves and relations between the pore size and capillary condensation pressure in these three methods is expected to provide much more reliable results than the application of the BdB method.

Although common for OOINs, [2,12,46−48] the use of the HK method[103] or its various modifications[104] is strongly discouraged. In some cases, these approaches are capable of correctly reproducing the mesopore size,[93] but this is a result of the choice of parameters rather than their sound theoretical basis. The HK method does not capture the actual nature of adsorption in mesopores (multilayer adsorption followed by capillary condensation), but tacitly assumes that the initially empty pores become completely filled at relative pressures that are related to their size.[114] This assumption is also incorrect in the micropore range for which the method was originally developed.[115] Thus, the HK method and its modifications are notorious in producing artifacts,[114−116] such as prominent peaks in the micropore range for essentially mesoporous materials.[114,115] The artificial nature of these peaks was recognized by some materials scientists,[12] but their appearance may be misleading for others. Thus, the use of the HK method is strongly discouraged, unless one is able to separate the actual information from the many artifacts.

In this section, the methodology for accurate PSD calculations for OOINs with cylindrical pore geometry, which is most common for these materials, was discussed. For other OOIN pore geometries, one can use the methods for cylindrical pores, although the pore size assessment would be less accurate and some artifacts may appear on PSDs. Alternatively, methods to calculate PSDs for other pore geometries, such as slit-like,[117−119] or spherical,[120] can be employed, but some of these methods were developed for materials with surfaces of properties largely different from those of OOINs (for instance, carbon surfaces),[117,119] and none of them was tested using model adsorbents. So their reliability for OOINs is uncertain. The discussion about PSD calculations was restricted to N_2 and Ar adsorbates. Some other adsorbates may also be useful in PSD calculations, but their adsorption behavior is less well understood. However, in the case of adsorbates such as

water or benzene that are capable of interacting in a more specific way with the OOINs surface, the feasibility of PSD determination is questionable because surface properties rather than PSD may have a predominant effect on adsorption behavior, as seen from recent studies.[44,46,48,53]

Characterization of Surface Properties

The ability of adsorbates to discriminate between inorganic and organic surfaces has long been recognized.[18,121−128] Early work was done largely on silica surfaces modified by esterification[18,122,128] or chemical bonding of organosilanes.[18,121,123−127] These surface modifications often led to dramatic changes in the adsorption behavior, which manifested itself in a significant decrease in the amount adsorbed (sometimes by more than 1 order of magnitude)[18,121,123] and adsorption energy,[121−123] and in the transition from Type II to Type III adsorption behavior.[124,126] Adsorption of polar molecules, such as water,[123−127] methanol,[123] triethylamine,[127] and some rather large nonpolar molecules, such as benzene,[121,123] hexane,[123] and carbon tetrachloride,[123] was particularly affected by introduction of hydrophobic organic groups on the silica surface. These findings constitute a good basis for a qualitative assessment of the surface properties of organic-modified silica surfaces. Moreover, in some cases, a more quantitative characterization could be made, including the assessment of the surface concentration of silanol groups using triethylamine adsorption.[127] Water adsorption has already been employed in OOIN studies.[38,44,46,48,49,53,55] Unmodified silica OMMs exhibited Types IV[38,44,49,53] or V[46,48] adsorption isotherms that changed to Type V[38,49] (from Type IV) or III[44,46,48,53] after chemical bonding of organosilanes or esterification. This was accompanied by a decrease in the water uptake. These changes were clearly correlated with the size[46,48] and structure[48] of the organic groups introduced. Surfaces of OOINs have also been studied using adsorption of benzene,[44,53] *n*-hexane, acetone, and methanol.[53] Adsorption of *n*-hexane was enhanced after surface modification with organic groups, whereas adsorption of benzene, acetone, and methanol was reduced. Phenyl-modified silica exhibited markedly different adsorption of *n*-butanol and *tert*-butyl alcohol, as adsorption of more bulky alcohol took place at lower relative pressures and with higher final uptake.[55]

Nitrogen adsorption was reported to be influenced by the presence of surface organic groups to a much smaller extent than adsorption of polar or large nonpolar molecules (see ref 18, p 699 for an account of Kiselev's work). However, nitrogen adsorption was found to have some important advantages, including the possibility of qualitative estimation of the strength of adsorbent−adsorbate interactions[84,85,122,126,128] or even calculation of the enthalpy of adsorption[122] on the basis of the BET *C*-constant.[64,66,68] This approach was employed in the OOIN studies. [42,56,57] Moreover, a method to evaluate the organic matter coverage on mineral surfaces was proposed on the basis of the enthalpy of adsorption evaluated from the BET *C*-constant.[129] Although the value of *C* is useful in a comparison of the surface properties, the calculation of the adsorption enthalpy from it is not recommended because of the approximate

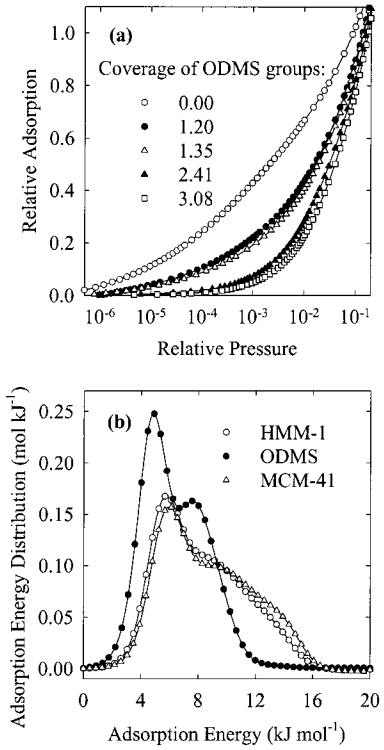

Figure 5. (a) Relative adsorption curves for silicas modified with different coverages of ODMS ligands. (b) Adsorption energy distributions for ethane silica PMO (HMM-1),[31] ODMS-modified MCM-41,[45] and siliceous MCM-41.[31] Data taken from refs 31, 59, and 45.

nature of the BET model (ref 68, p 102). Moreover, surfaces of appreciably different adsorption properties with respect to N_2 (such as those of MCM-41 modified with trimethylsilyl, butyldimethylsilyl, and polymeric octylsilyl)[45] may provide very similar BET *C*-constants, thus suggesting similarity for significantly different surfaces.

Despite these ambiguities, the information from the BET analysis, such as the specific surface area[90,121,126] or the monolayer capacity,[130] is useful in the analysis of surface properties of materials. Namely, it allows one to recalculate the adsorption isotherms so that they express the adsorption per unit area or the number of statistical layers on the surface (which will be referred to as relative adsorption), which opens many new opportunities in adsorption data interpretation. In particular, relative adsorption curves for samples modified with the same type of chemically bonded organic ligand, but with different surface coverage, are expected to gradually decrease in the low-pressure range as the surface coverage increases.[59] This behavior is illustrated in Figure 5a for ODMS-modified silicas. This finding suggests the possibility of development of a simple methodology to calculate the surface coverage of bonded groups from low-pressure nitrogen adsorption data.[59] A similar decrease in low-pressure adsorption was observed with the increase in the loading of organic molecules coated or chemically bonded on the silica surface, although in the case of a similar surface coverage, the chemical bonding had a larger effect on low-pressure adsorption, presumably because of a more uniform coverage and removal of strongly interacting sites during the chemical modification.[130] On the basis of the low-pressure adsorption data, it was possible to

evaluate the fraction of the surface coated by the organic modifier by employing bare silica surface as well as a chemically bonded and subsequently coated surface as references. This, in combination with elemental analysis data, allowed us to demonstrate that the coated layer on the MCM-41 surface was highly nonuniform,[50,51] whereas a satisfactory uniformity of coverage was observed for conventional silicas with significantly larger pores.[130] Nitrogen and argon relative adsorption curves for different bonded groups of the same surface coverage were found to be appreciably different, when the groups were dissimilar[45,62] and close to one another when the groups were similar.[131] The use of a comparative method to analyze low-pressure adsorption data also allows one to study surface properties[90,91] and organic groups on the silica surface in particular.[51,52,62] The theoretical foundations of this analysis were recently outlined to facilitate the prospective applications.[91] When silica is used as a reference adsorbent, the presence of organic groups on the surface of mesoporous silica results in downward deviations from linearity on the comparative plot. The extent of these deviations is dependent on the type of organic surface groups[51] and on their surface coverage. On the other hand, when a reference adsorption isotherm for strongly hydrophobic surfaces is used to analyze adsorption data for somewhat more polar surfaces, upward deviations of the comparative plot are observed.[52]

A very useful methodology to analyze low-pressure N_2 and Ar data is based on the calculation of adsorption energy distributions (AEDs).[66,132,133] AEDs were found to provide information about the presence of different surface groups, such as silanols, aliphatic groups, aromatic rings, and so forth, on the surface of modified silica.[45,51] Obviously, the information is obtained only about groups that are accessible to the adsorbate, and for instance silanol groups covered by a dense chemically bonded[45] or coated layer[130] will not be detected. In combination with elemental analysis data, AEDs may constitute the basis for evaluation of uniformity of the distribution of bonded organic ligands on the OOIN surface.[60] This was demonstrated in the case of trimethylsilyl ligands bonded on the MCM-41 surface using two different modification procedures, one on the calcined sample and the other one on the as-synthesized sample. The AEDs for the modified materials suggested that the distribution of bonded ligands was more uniform in the second case, as expected from the fact that organosilane is likely to displace electrostatically bonded surfactant ions that are likely to be uniformly distributed on the silicate surface. Illustrative AEDs are shown in Figure 5b. It can be seen that siliceous MCM-41 has very similar adsorption properties to ethane−silica PMO[31] and very different ones from ODMS-modified MCM-41.[45] This can be attributed to the fact that ethane−silica differs from silica only by substitution of some of the siloxane bridges by ethane groups, both of which are expected to interact weakly with nitrogen, resulting in similar nitrogen adsorption properties.[31] In contrast, the surface of an ODMS-modified sample has its surface effectively covered by octyl chains that interact with nitrogen very weakly.[45] Consistent information can be extracted from AEDs calculated on the basis of both N_2 and Ar data, showing the sensitivity of the latter gas to the surface properties of OOINs.[62] It should be noted that the exact shape of AED is somewhat model-dependent because of the many assumptions involved in the AED calculations.[89,132] Therefore, in the case of comparative studies, it is important to calculate AEDs consistently using the same set of parameters, the same model of adsorption behavior, and the same computational procedure.

Conclusions

There are many opportunities in gas adsorption characterization of OOINs. Adsorption data can be analyzed to evaluate the specific surface area, pore volume, and pore size distribution and to study the surface properties, all based for instance on a single nitrogen or argon adsorption isotherm measured in both low-pressure and high-pressure ranges. However, appropriate data analysis methods need to be used to avoid gross inaccuracies and artifacts. With these precautions, adsorption methods will be invaluable in the development of OOINs and in tailoring their structures toward intended applications.

Acknowledgment. The authors gratefully acknowledge the National Science Foundation (Grant CTS-0086512) and the donors of the Petroleum Research Fund administered by the American Chemical Society for support of this research.

References

(1) Yanagisawa, T.; Shimizu, T.; Kuroda, K.; Kato, C. *Bull. Chem. Soc. Jpn.* **1990**, *63*, 988.
(2) Beck, J. S.; Vartuli, J. C.; Roth, W. J.; Leonowicz, M. E.; Kresge, C. T.; Schmitt, K. D.; Chu, C. T.−W.; Olson, D. H.; Sheppard, E. W.; McCullen, S. B.; Higgins, J. B.; Schlenker, J. L. *J. Am. Chem. Soc.* **1992**, *114*, 10834.
(3) Stein, A.; Melde, B. J.; Schroden, R. C. *Adv. Mater.* **2000**, *12*, 1403.
(4) Asefa, T.; Yoshina-Ishii, C.; MacLachlan, M. J.; Ozin, G. A. *J. Mater. Chem.* **2000**, *10*, 1751.
(5) Huo, Q.; Margolese, D. I.; Ciesla, U.; Demuth, D. G.; Feng, P.; Gier, T. E.; Sieger, P.; Firouzi, A.; Chmelka, B. F.; Schuth, F.; Stucky, G. D. *Chem. Mater.* **1994**, *6*, 1176.
(6) Burkett, S. L.; Sims, S. D.; Mann, S. *Chem. Commun.* **1996**, 1367.
(7) Macquarrie, D. J. *Chem. Commun.* **1996**, 1961.
(8) Richer, R.; Mercier, L. *Chem. Commun.* **1998**, 1775.
(9) Markowitz, M. A.; Klaehn, J.; Hendel, R. A.; Qadriq, S. B.; Golledge, S. L.; Castner, D. G.; Gaber, B. P. *J. Phys. Chem. B* **2000**, *104*, 10820.
(10) Margolese, D.; Melero, J. A.; Christiansen, S. C.; Chmelka, B. F.; Stucky, G. D. *Chem. Mater.* **2000**, *12*, 2448.
(11) Yanagisawa, T.; Shimizu, T.; Kuroda, K.; Kato, C. *Bull. Chem. Soc. Jpn.* **1990**, *63*, 1535.
(12) Vartuli, J. C.; Schmitt, K. D.; Kresge, C. T.; Roth, W. J.; Leonowicz, M. E.; McCullen, S. B.; Hellring, S. D.; Beck, J. S.; Schlenker, J. L.; Olson, D. H.; Sheppard, E. W. *Chem. Mater.* **1994**, *6*, 2317.
(13) Antochshuk, V.; Jaroniec, M. *Chem. Commun.* **1999**, 2373.
(14) Antochshuk, V.; Jaroniec, M. *Chem. Mater.* **2000**, *12*, 2496.
(15) Lin, H.-P.; Yang, L.-Y.; Mou, C.-Y.; Liu, S.-B.; Lee, H.-K. *New J. Chem.* **2000**, *24*, 253.
(16) *Packings and Stationary Phases in Chromatographic Techniques*; Unger, K. K., Ed.; Marcel Dekker: New York, 1990.
(17) Vansant, E. F.; Van der Voort, P.; Vrancken, K. C. *Characterization and Modification of the Silica Surface*; Elsevier: Amsterdam, 1995.
(18) Iler, R. K. *The Chemistry of Silica*; Wiley: New York, 1979.
(19) Babonneau, F.; Leite, L.; Fontlupt, S. *J. Mater. Chem.* **1999**, *9*, 175.
(20) Raman, N. K.; Anderson, M. T.; Brinker, C. J. *Chem. Mater.* **1996**, *8*, 1682.
(21) Inagaki, S.; Guan, S.; Fukushima, Y.; Ohsuna, T.; Terasaki, O. *J. Am. Chem. Soc.* **1999**, *121*, 9611.

(22) Melde, B. J.; Holland, B. T.; Blanford, C. F.; Stein, A. *Chem. Mater.* **1999**, *11*, 3302.
(23) Asefa, T.; MacLachlan, M. J.; Coombs, N.; Ozin, G. A. *Nature* **1999**, *402*, 867.
(24) Lu, Y.; Fan, H.; Doke, N.; Loy, D. A.; Assink, R. A.; LaVan, D. A.; Brinker, C. J. *J. Am. Chem. Soc.* **2000**, *122*, 5258.
(25) Guan, S.; Inagaki, S.; Ohsuna, T.; Terasaki, O. *J. Am. Chem. Soc.* **2000**, *122*, 5660.
(26) Asefa, T.; MacLachlan, M. J.; Grondey, H.; Coombs, N.; Ozin, G. A. *Angew. Chem., Int. Ed.* **2000**, *39*, 1808.
(27) Yoshina-Ishii, C.; Asefa, T.; Coombs, N.; MacLachlan, M. J.; Ozin, G. A. *Chem. Commun.* **1999**, 2539.
(28) Shea, K. J.; Loy, D. A.; Webster, O. W. *Chem. Mater.* **1989**, *1*, 572.
(29) Loy, D. A.; Shea, K. J. *Chem. Rev.* **1995**, *95*, 1431.
(30) Cerveau, G.; Corriu, R. J. P. *Coord. Chem. Rev.* **1998**, *178*−*180*, 1051.
(31) Kruk, M.; Jaroniec, M.; Guan, S.; Inagaki, S. *J. Phys. Chem. B* **2001**, *105*, 681.
(32) Huo, Q.; Margolese, D. I.; Stucky, G. D. *Chem. Mater.* **1996**, *8*, 1147.
(33) Denoyel, R.; Sabio Rey, E. *Langmuir* **1998**, *14*, 7321.
(34) Jaroniec, M.; Kruk, M.; Shin, H. J.; Ryoo, R.; Sakamoto, Y.; Terasaki, O. *Microporous Mesoporous Mater.*, in press.
(35) Ryoo, R.; Park, I.-S.; Jun, S.; Lee, C. W.; Kruk, M.; Jaroniec, M. *J. Am. Chem. Soc.* **2001**, *123*, 1650.
(36) Kruk, M.; Jaroniec, M.; Sakamoto, Y.; Terasaki, O.; Ryoo, R.; Ko, C. H. *J. Phys. Chem. B* **2000**, *104*, 292.
(37) Kruk, M.; Jaroniec, M.; Ryoo, R.; Joo, S. H. *Chem. Mater.* **2000**, *12*, 1414.
(38) Park, M.; Komarneni, S. *Microporous Mesoporous Mater.* **1998**, *25*, 75.
(39) Zhao, H.; Nagy, K. L.; Waples, J. S.; Vance, G. F. *Environ. Sci. Technol.* **2000**, *34*, 4822.
(40) Kubota, Y.; Nishizaki, Y.; Sugi, Y. *Chem. Lett.* **2000**, 998.
(41) Sayari, A.; Yang, Y.; Kruk, M.; Jaroniec, M. *J. Phys. Chem. B* **1999**, *103*, 3651.
(42) Brunel, D.; Cauvel, A.; Fajula, F.; DiRenzo, F. *Stud. Surf. Sci. Catal.* **1995**, *97*, 173.
(43) Lim, M. H.; Blanford, C. F.; Stein, A. *J. Am. Chem. Soc.* **1997**, *119*, 4090.
(44) Zhao, Z. S.; Lu, G. Q. *J. Phys. Chem. B* **1998**, *102*, 1556.
(45) Jaroniec, C. P.; Kruk, M.; Jaroniec, M.; Sayari, A. *J. Phys. Chem. B* **1998**, *102*, 5503.
(46) Kimura, T.; Kuroda, K.; Sugahara, Y.; Kuroda, K. *J. Porous Mater.* **1998**, *5*, 127.
(47) Mercier, L.; Pinnavaia, T. J. *Environ. Sci. Technol.* **1998**, *32*, 2749.
(48) Kimura, T.; Saeki, S.; Sugahara, Y.; Kuroda, K. *Langmuir* **1999**, *15*, 2794.
(49) Van Der Voort, P.; Baltes, M.; Vansant, E. F. *J. Phys. Chem. B* **1999**, *103*, 10102.
(50) Jaroniec, M.; Kruk, M.; Jaroniec, C. P.; Sayari, A. *Adsorption* **1999**, *5*, 39.
(51) Kruk, M.; Jaroniec, M. In *Surfaces of Nanoparticles and Porous Materials*; Schwarz, J. A., Contescu, C., Eds.; Marcel Dekker: New York, 1999; p 443.
(52) Kruk, M.; Antochshuk, V.; Jaroniec, M.; Sayari, A. *J. Phys. Chem. B* **1999**, *103*, 10670.
(53) Zhao, X. S.; Lu, G. Q.; Hu, X. *Microporous Mesoporous Mater.* **2000**, *41*, 37.
(54) Mercier, L.; Pinnavaia, T. J. *Chem. Commun.* **2000**, *12*, 188.
(55) Bambrough, C. M.; Slade, R. C. T.; Williams, R. T. *Stud. Surf. Sci. Catal.* **2000**, *129*, 617.
(56) Brunel, D.; Sutra, P.; Fajula, F. *Stud. Surf. Sci. Catal.* **2000**, *129*, 773.
(57) Anwander, R.; Nagl, I.; Widenmeyer, M.; Engelhardt, G.; Groeger, O.; Palm, C.; Roser, T. *J. Phys. Chem. B* **2000**, *104*, 3532.
(58) Liu, J.; Shin, Y.; Nie, Z.; Chang, J. H.; Wang, L.-Q.; Fryxell, G. E.; Samuels, W. D.; Exarhos, G. J. *J. Phys. Chem. A* **2000**, *104*, 8328.
(59) Jaroniec, M.; Antochshuk, V.; Kruk, M. In *Adsorption Science and Technology*; Do, D. D., Ed.; World Scientific Publishers: New Jersey, 2000; p 299.
(60) Antochshuk, V.; Jaroniec, M. *Stud. Surf. Sci. Catal.* **2000**, *129*, 265.
(61) Ryoo, R.; Ko, C. H.; Kruk, M.; Antochshuk, V.; Jaroniec, M. *J. Phys. Chem. B* **2000**, *104*, 11465.
(62) Kruk, M.; Jaroniec, M. *Microporous Mesoporous Mater.* **2001**, *44*−*45*, 725.
(63) Brunel, D.; Cauvel, A.; Di Renzo, F.; Fajula, F.; Fubini, B.; Onida, B.; Garrone, E. *New. J. Chem.* **2000**, *24*, 807.
(64) Gregg, S. J.; Sing, K. S. W. *Adsorption, Surface Area and Porosity*; Academic Press: London, 1982.
(65) Sing, K. S. W.; Everett, D. H.; Haul, R. A. W.; Moscou, L.; Pierotti, R. A.; Rouquerol, J.; Siemieniewska, T. *Pure Appl. Chem.* **1985**, *57*, 603.
(66) Jaroniec, M.; Madey, R. *Physical Adsorption on Heterogeneous Solids*; Elsevier: Amsterdam, 1988.
(67) Rouquerol, J.; Avnir, D.; Fairbridge, C. W.; Everett, D. H.; Haynes, J. H.; Pernicone, N.; Ramsay, J. D. F.; Sing, K. S. W.; Unger, K. K. *Pure Appl. Chem.* **1994**, *66*, 1739.
(68) Rouquerol, F.; Rouquerol, J.; Sing, K. *Adsorption by Powders and Porous Solids*; Academic Press: San Diego, 1999.
(69) Kruk, M.; Jaroniec, M. *Chem. Mater.* **2000**, *12*, 222.
(70) Franke, O.; Schulz-Ekloff, G.; Rathousky, J.; Starek, J.; Zukal, A. *J. Chem. Soc., Chem. Commun.* **1993**, 724.
(71) Branton, P. J.; Hall, P. G.; Sing, K. S. W.; Reichert, H.; Schuth, F.; Unger, K. K. *J. Chem. Soc., Faraday Trans.* **1994**, *90*, 2965.
(72) Ball, P. C.; Evans, R. *Langmuir* **1989**, *5*, 714.
(73) Maddox, M. W.; Lastoskie, C. M.; Quirke, N.; Gubbins, K. E. In *Fundamentals in Adsorption*, LeVan, M. D., Ed.; Kluwer: Boston, 1996; p 571.
(74) Liu, H.; Zhang, L.; Seaton, N. A. *J. Colloid Interface Sci.* **1993**, *156*, 285.
(75) Ravikovitch, P. I.; Domhnaill, S. C. O.; Neimark, A. V.; Schüth, F.; Unger, K. K. *Langmuir* **1995**, *11*, 4765.
(76) Kruk, M.; Jaroniec, M.; Sayari, A. *Langmuir* **1997**, *13*, 6267.
(77) Zhao, D.; Yang, P.; Melosh, N.; Feng, J.; Chmelka, B. F.; Stucky, G. D. *Adv. Mater.* **1998**, *10*, 1380.
(78) Yu, C.; Yu, Y.; Zhao, D. *Chem. Commun.* **2000**, 575.
(79) Lukens, W. W., Jr.; Yang, P.; Stucky, G. D. *Chem. Mater.* **2001**, *13*, 28.
(80) Lin, H.-P.; Wong, S.-T.; Mou, C.-Y.; Tang, C.-Y. *J. Phys. Chem. B* **2000**, *104*, 8967.
(81) Kooyman, P. J.; Verhoef, M. J.; Prouzet, E. *Stud. Surf. Sci. Catal.* **2000**, *129*, 535.
(82) Kruk, M.; Jaroniec, M.; Yang, Y.; Sayari, A. *J. Phys. Chem. B* **2000**, *104*, 1581.
(83) Brunauer, S.; Emmett, P. H.; Teller, E. *J. Am. Chem. Soc.* **1938**, *60*, 309.
(84) Jelinek, L.; sz. Kovats, E. *Langmuir* **1994**, *10*, 4225.
(85) Amati, D.; sz. Kovats, E. *Langmuir* **1987**, *3*, 687.
(86) Avnir, D.; Farin, D.; Pfeifer, P. *New J. Chem.* **1992**, *16*, 439.
(87) Jaroniec, M.; Kruk, M.; Olivier, J. P. *Langmuir* **1999**, *15*, 5410.
(88) Dabadie, T.; Ayral, A.; Guizard, C.; Cot, L.; Lacan, P. *J. Mater. Chem.* **1996**, *6*, 1789.
(89) Kruk, M.; Jaroniec, M.; Sayari, A. *J. Phys. Chem. B* **1997**, *101*, 583.
(90) Karnaukhov, A. P.; Fenelonov, V. B.; Gavrilov, V. Y. *Pure Appl. Chem.* **1989**, *61*, 1913.
(91) Jaroniec, M.; Kaneko, K. *Langmuir* **1997**, *13*, 6589.
(92) Bhambhani, M. R.; Cutting, P. A.; Sing, K. S. W.; Turk, D. H. *J. Colloid Interface Sci.* **1972**, 38, 109.
(93) Galarneau, A.; Desplantier, D.; Dutartre, R.; Di Renzo, F. *Microporous Mesoporous Mater.* **1999**, *27*, 297.
(94) Fenelonov, V. B.; Romannikov, V. N.; Derevyankin, A. Yu. *Microporous Mesoporous Mater.* **1999**, *28*, 57.
(95) Sonwane, C. G.; Bhatia, S. K. *J. Phys. Chem. B* **2000**, *104*, 9099.
(96) Barrett, E. P.; Joyner, L. G.; Halenda, P. P. *J. Am. Chem. Soc.* **1951**, *73*, 373.
(97) Cranston, R. W.; Inkley, F. A. *Adv. Catal.* **1957**, *9*, 143.
(98) Dollimore, D.; Heal, G. R. J. *Appl. Chem.* **1964**, *14*, 109.
(99) Broekhoff, J. C. P.; de Boer, J. H. *J. Catal.* **1967**, *9*, 8.
(100) Broekhoff, J. C. P.; de Boer, J. H. *J. Catal.* **1967**, *9*, 15.
(101) Broekhoff, J. C. P.; de Boer, J. H. *J. Catal.* **1968**, *10*, 368.
(102) Broekhoff, J. C. P.; de Boer, J. H. *J. Catal.* **1968**, *10*, 377.
(103) Horvath, G.; Kawazoe, K. *J. Chem. Eng. Jpn.* **1983**, *16*, 470.
(104) Saito, A.; Foley, H. C. *AIChE J.* **1991**, *37*, 429.
(105) Jaroniec, M.; Choma, J.; Kruk, M., unpublished work.
(106) Lastoskie, C.; Gubbins, K. E.; Quirke, N. *J. Phys. Chem.* **1993**, *97*, 4786.
(107) Maddox, M. W.; Olivier, J. P.; Gubbins, K. E. *Langmuir* **1997**, *13*, 1737.
(108) Jaroniec, M.; Kruk, M.; Olivier, J. P.; Koch, S. *Stud. Surf. Sci. Catal.* **2000**, *128*, 71.
(109) Ravikovitch, P. I.; Wei, D.; Chueh, W. T.; Haller G. L.; Neimark, A. V. *J. Phys. Chem. B* **1997**, *101*, 3671.
(110) Ravikovitch, P. I.; Neimark, A. V. *Stud. Surf. Sci. Catal.* **2000**, *129*, 597.
(111) Kruk, M.; Jaroniec, M.; Sayari, A. *Adsorption* **2000**, *6*, 47.
(112) Lukens, W. W., Jr.; Schmidt-Winkel, P.; Zhao, D.; Feng, J.; Stucky, G. D. *Langmuir* **1999**, *15*, 5403.
(113) Zhao, D.; Huo, Q.; Feng, J.; Chmelka, B. F.; Stucky, G. D. *J. Am. Chem. Soc.* **1998**, *120*, 6024.
(114) Jaroniec, M.; Choma, J.; Kruk, M. *Stud. Surf. Sci. Catal.* **2000**, *128*, 225.
(115) Kruk, M.; Jaroniec, M.; Choma, J. *Adsorption* **1997**, *3*, 209.
(116) Kaminsky, R. D.; Maglara, E.; Conner, W. C. *Langmuir* **1994**, *10*, 1556.
(117) Olivier, J. P. *Carbon* **1998**, *36*, 1469.
(118) Olivier, J. P.; Occelli, M. L. *J. Phys. Chem. B* **2001**, *105*, 623.
(119) Ravikovitch, P. I.; Vishnyakov, A.; Russo, R.; Neimark, A. V. *Langmuir* **2000**, *16*, 2311.
(120) Broekhoff, J. C. P.; de Boer, J. H. *J. Catal.* **1968**, *10*, 153.
(121) Kiselev, A. V. *Quart. Rev. Chem. Soc.* **1961**, *15*, 99.

(122) Lowen, W. K.; Broge, E. C. *J. Phys. Chem.* **1961**, *65*, 16.
(123) Kiselev, A. V. *J. Colloid Interface Sci.* **1968**, *28*, 430.
(124) Alzamora, L.; Contreras, S.; Cortes, J. *J. Colloid Interface Sci.* **1975**, *50*, 503.
(125) Zettlemoyer, A. C.; Hsing, H. H. *J. Colloid Interface Sci.* **1977**, *58*, 263.
(126) Barraclough, P. B.; Hall, P. G. *J. Chem. Soc., Faraday Trans. 1* **1978**, *74*, 1360.
(127) Kiselev, A. V.; Kuznetsov, B. V.; Lanin, S. N. *J. Colloid Interface Sci.* **1979**, *69*, 148.
(128) Day, R. E.; Parfitt, G. D.; Peacock, J. *J. Colloid Interface Sci.* **1979**, *70*, 130.
(129) Mayer, L. M. *Geochim. Cosmochim. Acta* **1999**, *63*, 207.
(130) Kruk, M.; Jaroniec, M.; Gilpin, R. K.; Zhou, Y. W. *Langmuir* **1997**, *13*, 545.
(131) Jaroniec, C. P.; Gilpin, R. K.; Jaroniec, M. *J. Phys. Chem. B* **1997**, *101*, 6861.
(132) von Szombathely, M.; Brauer, P.; Jaroniec, M. *J. Comput. Chem.* **1992**, *13*, 17.
(133) Olivier, J. P. In *Fundamentals of Adsorption*; LeVan, M. D., Ed.; Kluwer: Boston, 1996; p 699.

CM0101069